U.S. DEPARTMENT OF THE INTERIOR

U.S. GEOLOGICAL SURVEY

Metal distribution in overbank sediments from the Alamosa River, south-central Colorado

by

K.C. Stewart*, P.H. Briggs*, D.L. Fey*, M.J. Malcolm*, and A.L. Meier*

Open-File Report 95-643

*U.S. Geological Survey, Box 25046, MS 973, Denver Federal Center, Denver, CO 80225

1995

CONTENTS

TABLES

FIGURES

APPENDIX TABLES

ABSTRACT

After broken pipelines and springs beneath a heap leach leaked substantial amounts of acidic metal-bearing solutions into the Wightman Fork below the Summitville open-pit gold mine in south-central Colorado, a study was undertaken to determine the metal distribution in overbank sediments along the Alamosa River. The purpose of the study was to statistically investigate the effect of the Wightman Fork on total sediment chemistry and to determine if dissolution of metal salts in oxidized sediments could contribute to the lower pH and higher dissolved metal load in the Alamosa River after storms. Overbank sediments were collected along the Alamosa River from its headwaters to Terrace Reservoir and the <0.25 mm fraction was analyzed for total and water-extractable metal content.

Results of the study indicate that the Wightman Fork is the major source of solid-phase and water-extractable copper in overbank sediments along the Alamosa River. Lesser, but still significant, amounts of total arsenic and lead are found in sediments below the Wightman Fork, although the major increase of lead in sediments appears below Alum Creek. There were no significant increases in total iron, manganese, zinc, cobalt and nickel below the Wightman Fork compared to upstream. On the other hand, highly significant increases in water-extractable zinc and significant increases in extractable manganese were found below the Wightman Fork compared to upstream.

Metal concentrations in water extracts of overbank sediments suggest that dissolution of readily-soluble minerals in overbank sediments could contribute to the lowering of pH and the raising of dissolved metal loads in the Alamosa River after storms.

INTRODUCTION

The Alamosa River has been studied extensively since 1992 when a series of broken pipelines and springs beneath a heap leach that was constructed at the Summitville open-pit gold mine leaked substantial amounts of acidic metal-bearing solutions into the Wightman Fork, a tributary to the Alamosa River (Pendleton and others, 1995)(fig. 1). High concentrations of total copper, arsenic, and lead were found in sediments in the Wightman Fork in addition to high concentrations of dissolved copper in water just below the confluence of the Wightman Fork with the Alamosa River in June 1993 (Balistrieri and others, 1995). Sediment samples taken in the Wightman Fork had levels of arsenic and copper that were ten times higher than those in a sediment taken along the Alamosa River just above the confluence with the Wightman Fork. Another study showed a ten-times increase in levels of dissolved aluminum, copper and iron, and a significant drop in water pH after a storm event in the portion of the Alamosa River below Jasper Creek (Ortiz and others, 1995). Overbank sediments, which are deposited during floodstage outside normal stream channels, are exposed to conditions of oxidation and evaporation that favor formation of secondary metal salts. These secondary minerals contain potential reservoirs of metals and acidity that could become mobilized during storm events. The purpose of this study was to learn the distribution and total concentration of metals in overbank sediments along the Alamosa River and to determine water-extractable concentrations of metals as a measure of whether storm events might lower the pH and increase the dissolved metal loads

in the Alamosa River by dissolution of soluble metal salts.

FIELD SAMPLING

An unbalanced, three-level, stratified sampling design was used to assess variation of element concentrations in overbank sediments from the Alamosa River. Samples were taken at approximately 1-mile intervals from Terrace Reservoir upstream to Asiatic Creek (fig. 1). Treasure Creek and Gold Creek (which form the headwaters of the Alamosa River) were also sampled at sites outside the primary altered area of the Platoro Caldera (Lipman, 1974). At each location two samples were collected roughly 60 m apart to assess variability within each site. All samples were taken on the north and west side of the river or its tributaries. Samples were collected on sand bars and floodplains bordering the active channel. At each site the downstream sample was collected first, then the upstream sample. The upper 5 cm of surface sediment was composited from several locations and a subsample was placed in paper bags for transport to the laboratory.

SAMPLE PREPARATION

Sediment samples were air dried in the laboratory at ambient room temperature (about 20° C), sieved to pass a 60-mesh (0.25 mm) stainless-steel screen, and ground to pass a 100-mesh (0.15 mm) screen. Eight randomly-selected samples (20%) were split to assess variability of samples and analytical techniques. For determination of water-soluble constituents, sediments were extracted with unbuffered deionized water at pH 5.8 (1 part sediment:20 parts water, by weight) in 4-oz, acid-washed polypropylene bottles (Stewart and others, 1990). Sediment was kept in suspension by agitation on a horizontal reciprocating shaker for 16 hours at 58 oscillations per minute. Solutions were clarified by centrifugation at 15,000 rpm for 10 minutes, filtered through 0.45 μm filters, and separated into two portions. One portion was acidified with nitric acid for soluble metal determination and the other portion was used for determination of specific conductance and pH.

ANALYTICAL TECHNIQUES

Total element concentrations were determined by inductively-coupled argon plasma-atomic emission spectroscopy (ICP-AES) after decomposition with a multi-acid digestion (Crock and others, 1983; Briggs, 1990). Total arsenic was determined by flow injection hydride-generation-atomic absorption spectroscopy (HGAAS, Crock and Lichte, 1982; Sanzolone and Chao, 1987; Welsch,1990). Soluble metals in the extracts were determined by inductively-coupled argon plasma-mass spectroscopy (ICP-MS, Meier and others, 1994). Specific conductance of the extracts was measured at room temperature by conductivity meter and pH determinations were made by pH meter. Table 1 lists determination limits for elements reported by each technique.

RESULTS AND DISCUSSION

Table 2 presents results of analysis of variance (ANOVA) for total element concentrations in overbank sediments. Position above or below the Wightman Fork accounted for the highest proportion of the total variability in copper, arsenic, and lead. A smaller, but still significant percentage of variance was found among the sample sites. The percentage of variance between samples within sites for these elements was less than 5%, which means that distribution of these elements was relatively uniform over areas as large as 60 m.

Figure 2 plots mean total copper and arsenic in Alamosa River overbank sediments versus river miles. Terrace Reservoir dam is marked with an arrow on the X-axis. Below the mouth of the Wightman Fork, copper concentrations are ten times higher than in sediments found above the Wightman Fork. Arsenic concentrations increase by two times below the mouth of the Wightman Fork. ANOVA and plots of the data indicate that the Wightman Fork is the major source of copper and arsenic to Alamosa River overbank sediments. For copper, this could result from low-pH, high-copper water coming into contact with higher-pH water in the Alamosa River causing sorption of copper onto hydrous iron oxides. Field studies have shown that at pH 6, 80 percent of copper in mine-drainage waters is associated with the particulate fraction (Smith and others, 1992). In the Wightman Fork, median pH's have ranged from 4.5-5.0 and median dissolved copper concentrations have ranged from 2250-8600 µg/L (Balistrieri and others, 1995, Walton-Day and others, 1995). In the Alamosa River, just below the confluence with the Wightman Fork, dissolved copper concentrations decreased to 700-1000 µg/L and pH's increased to 8.0. Enargite (Cu_3AsS_4), a common ore mineral at Summitville (Steven and Ratte, 1960), could be the source of copper and arsenic in the Wightman Fork if this mineral is abundant in the heap leach. Mechanical erosion of altered rocks exposed in the Summitville area could also be a source of copper and arsenic to the sediments. A copper-arsenic anomaly was found in Alamosa River floodplain sediments that extends into the San Luis Valley (Tidball and others, 1995).

Figure 3 shows concentrations of lead in overbank sediments. Although location above or below the Wightman Fork accounts for 83 percent of the total variance in lead concentrations, Alum Creek appears to be a more important source of lead to Alamosa River sediments than the Wightman Fork. Concentrations increase by a factor of three below the confluence with Alum Creek. The overall trend in lead concentration seems to be rising from the headwaters downstream to Terrace Reservoir. Sediments collected along the Alamosa River in 1994 by other investigators showed the same trend (Church and others, 1995).

The highest percentage of the total variance for iron, manganese, chromium, cobalt, nickel, vanadium and zinc was found among the individual sample sites. The percentage of variance accounted for by location above or below the Wightman Fork was significant only for manganese and chromium. Ten percent or less of the total variance for manganese and chromium was due to sample differences within sites. Within-site variance ranged from 18-24 percent of the total for iron, cobalt, nickel, vanadium and zinc, and was higher than the variance accounted for by position above or below the Wightman Fork. This means that for these elements, variability among individual sites is greater than differences found between sites above and below the Wightman Fork and reflects the geology of the entire drainage basin.

Total iron concentration doubles below Asiatic Creek compared to the two sites

upstream, and reaches its maximum concentration in sediments taken below Iron Creek (fig. 4). Iron concentration falls to near-background levels below Alum Creek. Total iron concentration rises again downstream to the Wightman Fork, but falls again to near background levels below the Wightman Fork. Total manganese concentration also decreases below Alum Creek (fig. 5), but in contrast to iron, manganese levels do not rise again to values found above Asiatic Creek. Mean concentrations of manganese are higher above the confluence of the Wightman Fork than below. Cobalt and zinc concentrations increase below Asiatic Creek (table A1, field # AR19).

Based on ANOVA calculations from samples analyzed in duplicate, the analytical component for total element concentrations was significant only for cerium.

Table 3 presents ANOVA results for the water-extractable constituents in the overbank sediments. Similar to results for total copper, position above or below the Wightman Fork accounts for a highly significant proportion of the total variance for water-extractable copper. This is the only level in the ANOVA design that accounts for a significant portion of the total variance, and indicates that the Wightman Fork is the major source of water-extractable copper associated with overbank sediments in the Alamosa River drainage basin. Water-extractable manganese and zinc are also found below the Wightman Fork, but differences among sample sites accounted for a highly significant proportion of the total variance for these two elements. For samples extracted in duplicate, ANOVA showed that the percentage of the total variance accounted for by the extraction and analytical component was not significant for these elements.

We interpret the data to indicate that dissolution of sorbed metals or metal salts associated with overbank sediments along the Alamosa River can cause a substantial increase in the load of dissolved copper, manganese and zinc during high flow associated with storm events. The loads for these three elements will increase substantially below the Wightman Fork. Figure 6 shows that water-extractable copper in sediments increases by a factor of 20 below the Wightman Fork. Extractable zinc and manganese increase 4-5 fold below the Wightman Fork, but substantial increases in extractable manganese also appear below Iron and Alum Creeks. Farther downstream, extractable manganese and zinc return to levels found above the Wightman Fork, but copper values remain at least 3-fold higher than those found above the Wightman Fork. Values for extractable copper in sediments immediately below the Wightman Fork are similar to those found in water samples from the Alamosa River above Terrace Reservoir after a rainstorm in August 1993 (Ortiz and others, 1995). Another study of North Clear Creek in central Colorado showed that manganese and zinc in the water column during low flow was associated primarily with the dissolved fraction (Davis and others, 1991). Batch desorption studies on bed sediments showed that zinc and manganese were 80-85 percent desorbed from the particulate fraction at pH 4.4. At the same pH, 50 percent of the copper remained associated with the particulate fraction.

Concentrations of extractable aluminum, barium, and magnesium were not significantly higher in sediments below the Wightman Fork than concentrations found in sediments above the Wightman Fork ($p<0.05$). Differences among samples accounted for the highest percent of the total variance for these elements. Figure 7 shows that some sites above the Wightman Fork had concentrations of water-extractable aluminum that were 4-5 times higher than values found in sediments taken immediately below the Wightman Fork. These data suggest that suspension of overbank sediments can contribute to the load of dissolved aluminum in the Alamosa River after

a storm event, but that the major input is above the Wightman Fork.

Water-extractable iron, arsenic, nickel, chromium and cobalt were not found above the determination limits (table 1). The fact that iron could not be detected in the extracts suggests that overbank sediments from the Alamosa River are not the major source of soluble iron in the Alamosa River measured by Ortiz and others (1995), where concentrations reached 1500 μg/L after a storm. A source for this dissolved iron could have been oxidized pyrite float in the streambed of Burnt Creek or pyritic soils exposed during debris flow activity (Miller and McHugh, 1994; Kirkham and others, 1995).

The only significant percent of the total variance for pH of extracts was found among sample sites. The pH of all extracts was acidic and varied from 4.2 to 6.2 (fig. 8, table A3). The pH drops from 6.1 to 4.9 below the inflow of Iron Creek, but rises again to 5.7 at the next site downstream. Below the inflow of Alum Creek, extract pH drops to 4.8, rises, and then drops to its lowest value of 4.5 below Bitter Creek. The area drained by Alum Creek is underlain by pyrite-rich bedrock and active debris flows deposit substantial pyritic soil during thunderstorms (Kirkham and others, 1995). Dissolution of oxidized pyrite minerals probably contributes to the pH drop in extracts of the sediments taken below Alum Creek. Although the pH drops transiently below the Wightman Fork, the general trend in extract pH rises downstream from Bitter Creek. Similar trends in pH were found along the Alamosa River from a synoptic sampling of water conducted in May 1993, although the range in pH was greater for the water samples than for our extracts (Walton-Day and others, 1995). Total and water-extractable manganese had the highest single element correlation coefficients with pH (0.75 and -0.69 respectively). Lower pH's of extracts were associated with higher concentrations of soluble manganese. The pH of extracts has been used to effectively predict concentrations of total dissolved metals in overbank sediments from the Clark Fork River in Montana (Nimick and Moore, 1991).

Specific conductance in the extracts ranged from 17-98 μS/cm (fig. 9, table A3). Differences were not significantly different above and below the Wightman Fork ($p<0.05$). Highly significant differences in conductance were found among sample sites--56 percent of the total variance was accounted for by these differences. Conductance increased in extracts of sediments taken downstream from the mouths of the most chemically degraded streams. Water-extractable manganese and barium showed the highest single-element correlation coefficients with specific conductance (0.72 and 0.78, respectively). In general, high specific conductances corresponded to low pH's. The highest conductances were found in extracts from sediments below Alum Creek and the Wightman Fork, and corresponded to drops in extract pH. Conductances were ten times lower than those observed in water samples from the Alamosa River after the storm in August 1993. This could show either that minerals exposed in the Burnt Creek drainage or readily-soluble salts in the soil zone were influencing the water chemistry. Potassium increased early in storm runoff following a storm event in the Absaroka Mountains in Wyoming (Miller and Drever, 1977).

SUMMARY

Data from this study of overbank sediments along the Alamosa River support the following conclusions:

- The Wightman Fork is the major source of solid-phase and water-extractable copper in overbank sediments along the Alamosa River. Concentrations are significantly higher in sediments below the Wightman Fork than in sediments above the Wightman Fork. Mean concentractions of both total and water-extractable copper are 10 times higher below the Wightman Fork than above the Wightman Fork.
- Significantly higher concentrations of total arsenic and lead are found in sediments below the Wightman Fork than above the Wightman Fork. The major increase in arsenic appears below the Wightman Fork, but the major increase of lead in sediments appears below Alum Creek. Lead concententration in sediments from the Alamosa River show a general rising trend from the headwaters downstream to Terrace Reservoir.
- Total iron, manganese, zinc, cobalt and nickel concentrations in sediments are not significantly higher below the Wightman Fork than upstream. The maximum concentrations of total iron and manganese are found above the Wightman Fork in sediments taken below Asiatic and Iron Creeks.
- Highly significant increases in concentrations of water-extractable zinc and significant increases in concentrations of water-extractable manganese were found below the Wightman Fork compared to upstream. The data indicate that the Wightman Fork is the major source of extractable zinc in sediments and a significant contributor of extractable manganese. Sediments below Iron and Alum Creeks also contribute significant water-extractable manganese to the basin.
- Concentrations of water-extractable aluminum, barium and magnesium were not significantly higher in sediments taken below the Wightman Fork than in sediments taken above the Wightman Fork.
- The highest mean pH of 6.2 was found in extracts of sediments taken immediately below Asiatic Creek. The lowest mean pH of 4.5 was found in extracts of sediments taken below Bitter Creek. Specific conductance of all extracts was less than 100 µS/cm and showed a high variability between samples within sample sites.
- Metal concentrations in water extracts of overbank sediments indicate that dissolution of readily-soluble minerals in overbank sediments could contribute to the lowering of pH and the raising of dissolved metal loads in the Alamosa River after storms.

ACKNOWLEDGEMENTS

The authors would like to thank R.R. Tidball for suggestions on the sampling design, S.E. Church and K.S. Smith for helpful comments on the manuscript, and S.E. Church for preparation of figure 1.

REFERENCES CITED

Balistrieri, L.S., Gough, L.P., Severson, R.C., and Archuleta, A., 1995, The biogeochemistry of wetlands in the San Luis Valley, Colorado: The effects of acid drainage from natural and mine sources, *in* Posey, H.H., Pendleton, J.A., and Van Zyl, D., eds., Proceedings: Summitville Forum '95: Colorado Geological Survey Special Publication 38, p. 219-226.

Briggs, P.H., 1990, Elemental analysis of geological material by inductively coupled plasma-atomic emission spectrometry, *in* Arbogast, B.F., ed., Quality assurance manual for the Branch of Geochemistry, U.S. Geological Survey: U.S. Geological Survey Open-File Report 90-668, p. 83-91.

Church, S.E., Wilson, S.A., and Briggs, P.H., 1995, Geochemical and lead-isotopic studies of stream and river sediments, Alamosa River basin, Colorado: U.S. Geological Survey Open-File Report 95-250, 73 p..

Crock, J.G., and Lichte, F.E., 1982, An improved method for the determination of trace levels of arsenic and antimony in geologic materials by automated hydride generation-atomic absorption spectroscopy: Analytica Chimica Acta, v. 144, p. 223-233.

Crock, J.G., and Lichte, F.E., and Briggs, P.E., 1983, Determination of elements in National Bureau of Standards Geologic Reference Materials SRM 278 obsidian and SRM 688 basalt by inductively coupled argon plasma-atomic emission spectrometry: Geostandards Newsletter, v. 7, p. 335-340.

Davis, A., Olsen, R.L., and Walker, D.R., 1991, Distribution of metals between water and entrained sediment in streams impacted by acid mine discharge, Clear Creek, Colorado, U.S.A.: Applied Geochemistry, v. 6, p. 333-348.

Kirkham, R.M., Lovekin, J.R., and Sares, M.A., 1995, Sources of acidity and heavy metals in the Alamosa River basin outside of the Summitville mining area, Colorado, *in* Posey, H.H., Pendleton, J.A., and Van Zyl, D., eds., Proceedings: Summitville Forum '95: Colorado Geological Survey Special Publication 38, p. 42-57.

Lipman, P.W., 1975, Evolution of the Platoro caldera complex and related volcanic rocks, southwestern San Juan Mountains, Colorado: U.S. Geological Survey Professional Paper 852, 128 p.

Meier, A.L., Grimes, D.J., and Ficklin, W.H., 1994, Inductively coupled plasma mass spectrometry; a powerful analytical tool for mineral resources and environmental studies: U.S. Geological Survey Circular 1103-A, p. 67-68.

Miller, W.R., and Drever, J.I., 1977, Water chemistry of a stream following a storm, Absaroka Mountains, Wyoming: Geol. Soc. of America Bulletin, v. 88, p. 286-290.

Miller, W.R., and McHugh, J.B., 1994, Natural acid drainage from altered areas within and adjacent to the Upper Alamosa River Basin, Colorado: U.S. Geological Survey Open-File Report 94-144, 47 p.

Nimick, D., and Moore, J.N., 1991, Prediction of water-soluble metal concentrations in fluvially deposited tailings sediments, Upper Clark Fork Valley, Montana, U.S.A.: Applied Geochemistry, v. 6, p. 635-646.

Ortiz, R.F., von Guerard, P., and Walton-Day, K, 1995, Effect of a localized rainstorm on the

water quality of the Alamosa River upstream from terrace reservoir, south-central Colorado, August 9-10, 1993, *in* Posey, H.H., Pendleton, J.A., and Van Zyl, D., eds., Proceedings: Summitville Forum '95: Colorado Geological Survey Special Publication 38, p. 178-182.

Pendleton, J.A., Posey, H.H., and Long, M.B., 1995, Characterizing Summitville and its impacts: Setting the scene, *in* Posey, H.H., Pendleton, J.A., and Van Zyl, D., eds., Proceedings: Summitville Forum '95: Colorado Geological Survey Special Publication 38, p. 1-12.

Sanzolone, R.F., and Chao, T.T., 1987, Determination of selenium in thirty-two geochemical reference materials by continuous-flow hydride generation atomic absorption spectrophotometry: Geostandards Newsletter, v. 11, p. 81-85.

Smith, K.S., Ficklin, W.H., Plumlee, G.S., and Meier, A.L., 1992, Metal and arsenic partitioning between water and suspended sediment at mine-drainage sites in diverse geologic settings, *in* Kharaka, Y.K., and Maest, A.S., eds., Water-Rock Interaction: Rotterdam, A.A. Balkema, p. 443-447.

Steven, T.A., and Ratté, J.C., 1960, Geology and ore deposits of the Summitville District, San Juan Mountains, Colorado: U.S. Geological Survey Professional Paper 343, 70 p.

Stewart, K.C., Fey, D.L., Dunlap, C.E., and Welsch, E.P., 1990, Water-extractable elements from the Panoche Fan area of the San Joaquin Valley, California: U.S. Geological Survey Open-File Report 90-292, 24 p.

Tidball, R.R., Stewart, K.C., Tripp, R.B., and Mosier, E.L., 1995, Geochemical mapping of surficial materials in the San Luis, Valley, Colorado, *in* Posey, H.H., Pendleton, J.A., and Van Zyl, D., eds., Proceedings: Summitville Forum '95: Colorado Geological Survey Special Publication 38, p. 244-262.

Walton-Day, K, Ortiz, R.F.,and von Guerard, P., 1995, Sources of water having low pH and elevated metal concentrations in the upper Alamosa River from the headwaters to the outlet of Terrace Reservoir, south-central Colorado, April-September, 1993, *in* Posey, H.H., Pendleton, J.A., and Van Zyl, D., eds., Proceedings: Summitville Forum '95: Colorado Geological Survey Special Publication 38, p. 160-170.

Welsch, E.P., Crock, J.G., and Sanzolone, R., 1990, Determination of arsenic and selenium using continuous-flow hydride generation atomic absorption spectrophotometry, *in* Arbogast, B.F., ed., Quality assurance manual for the Branch of Geochemistry, U.S. Geological Survey: U.S. Geological Survey Open-File Report 90-668, p. 38-45.

Table 1. Analytical techniques, determination limits (DL), and reporting units for elements determined in overbank sediments from Alamosa River. DL for water-extractable constituents are reported in solution.

Method	DL, reporting units	Variables
Inductively-coupled argon plasma-atomic emission spectroscopy (ICP-AES)*	.05%	Al, Ca, Fe, K, Mg, Na, P, Ti
	100 ppm	U
	40 ppm	Ta
	10 ppm	As, Bi
	8 ppm	Au
	5 ppm	Sn
	4 ppm	Ce, Ga, Ho, Mn, Nb, Pb, Th, Zn
	2 ppm	Ag, Cd, La, Li, Mo, Ni, Sc, Sr, V, Y
Hydride-generation atomic absorption spectroscopy (HGAAS)*	0.1 ppm	As
Inductively-coupled argon plasma-mass spectroscopy (ICP-MS)¶	100 ppb	Fe
	3 ppb	Ni
	2 ppb	As, Zn
	1 ppb	Al, Cr, Mg
	0.2 ppb	Cu, Mn
	0.1 ppb	Ba, Co
pH meter¶	standard units	pH
Conductivity meter¶	µS/cm	specific conductance

* reported on a dry weight basis
¶ reported in solution

Table 2. Analysis of variance for elements measured in overbank sediments of the Alamosa River. Variance components were computed from log data unless otherwise noted. Arsenic was determined by hydride-generation atomic absorption spectroscopy (HGAAS). Other elements were determined by inductively-coupled argon plasma-atomic emission spectroscopy (ICP-AES).

		Percentage of variance		
Variable, units	Log_{10} total variance	above vs. below Wightman Fork	among sample sites	between samples within sample sites
Al, %	.00108	30*	60**	10
Ca, %	.06178	63**	35**	2
Fe, %	.00799	<1	76**	24
K, %¶	.00202	33*	60**	7
Mg, %	.01048	48**	50**	2
Na, %	.00949	<1	96**	4
P, %	.00076	11	44**	45
Ti, %	.01131	<1	83**	17
As, ppm¶	.27682	94**	5**	1
Ba, ppm¶	.04909	32*	40**	28
Be, ppm	.02895	49**	28**	23
Ce, ppm	.00166	<1	41*	59
Co, ppm	.01117	12	68**	20
Cr, ppm	.02192	33*	57**	10
Cu, ppm	.51795	98**	2**	<1
Mn, ppm	.02107	30*	62**	8
Ni, ppm¶	.00847	15	58**	27
Pb, ppm¶	.11882	83**	12**	5
Sc, ppm¶	.00406	55**	39**	6
Sr, ppm	.00609	8	89**	3
Th, ppm¶	.01388	19*	12	69
V, ppm	.01118	<1	82**	18
Y, ppm	.01326	39*	56**	5
Zn, ppm	.01456	5	76**	19

*Statistically significant at the 0.05 probability level

**Statistically significant at the 0.01 probability level

¶ Variance components computed from raw data, skewness and kurtosis show that raw data is closer to normal distribution than log data

Table 3. Site and analytical variance for elements measured in water extracts (1:20 sediment:water, by weight) of overbank sediments from the Alamosa River. Variance components were computed from log data unless otherwise noted. Metals were determined by inductively-coupled argon plasma mass spectroscopy (ICP-MS). Specific conductance (SC) was measured by conductivity meter and pH by pH meter.

		Percentage of variance		
Variable, units	Log_{10} total variance	above vs. below Wightman Fork	among sample sites	between samples within sample sites
Al, ppb	.17314	16	73**	11
Ba, ppb¶	.05159	19	51**	30
Cu, ppb	.62263	85**	2	13
Mg, ppb	.02225	5	59**	35
Mn, ppb¶	.15830	27*	65**	8
Zn, ppb	.14737	58**	23**	19
pH, units¶	.21458	12	61**	26
SC, µS/cm¶	.03408	2	44**	54

*Statistically significant at the 0.05 probability level

**Statistically significant at the 0.01 probability level

¶Variance components computed from raw data, skewness and kurtosis show that raw data is closer to normal distribution than log data

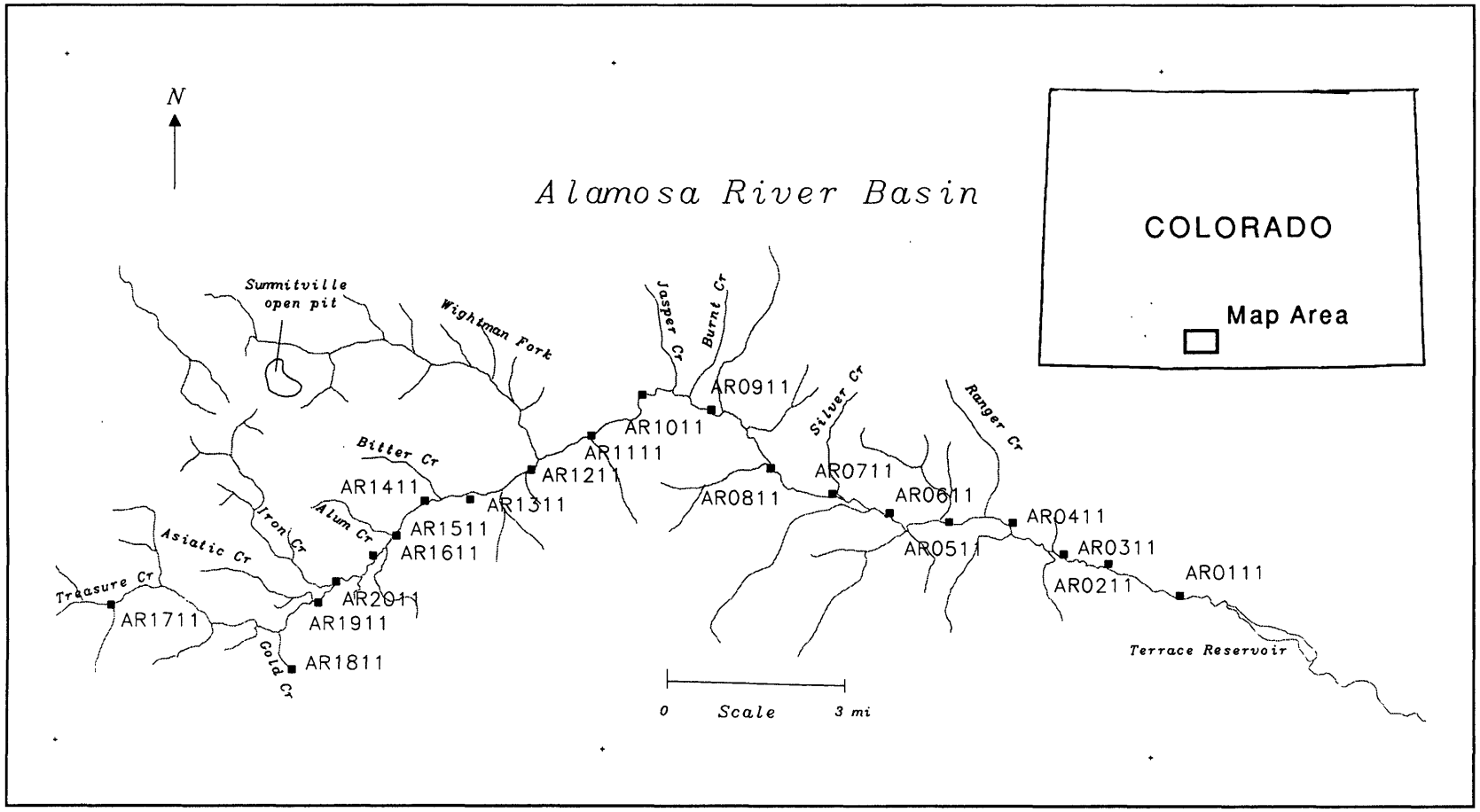

Figure 1. Index map of study area showing sample localities

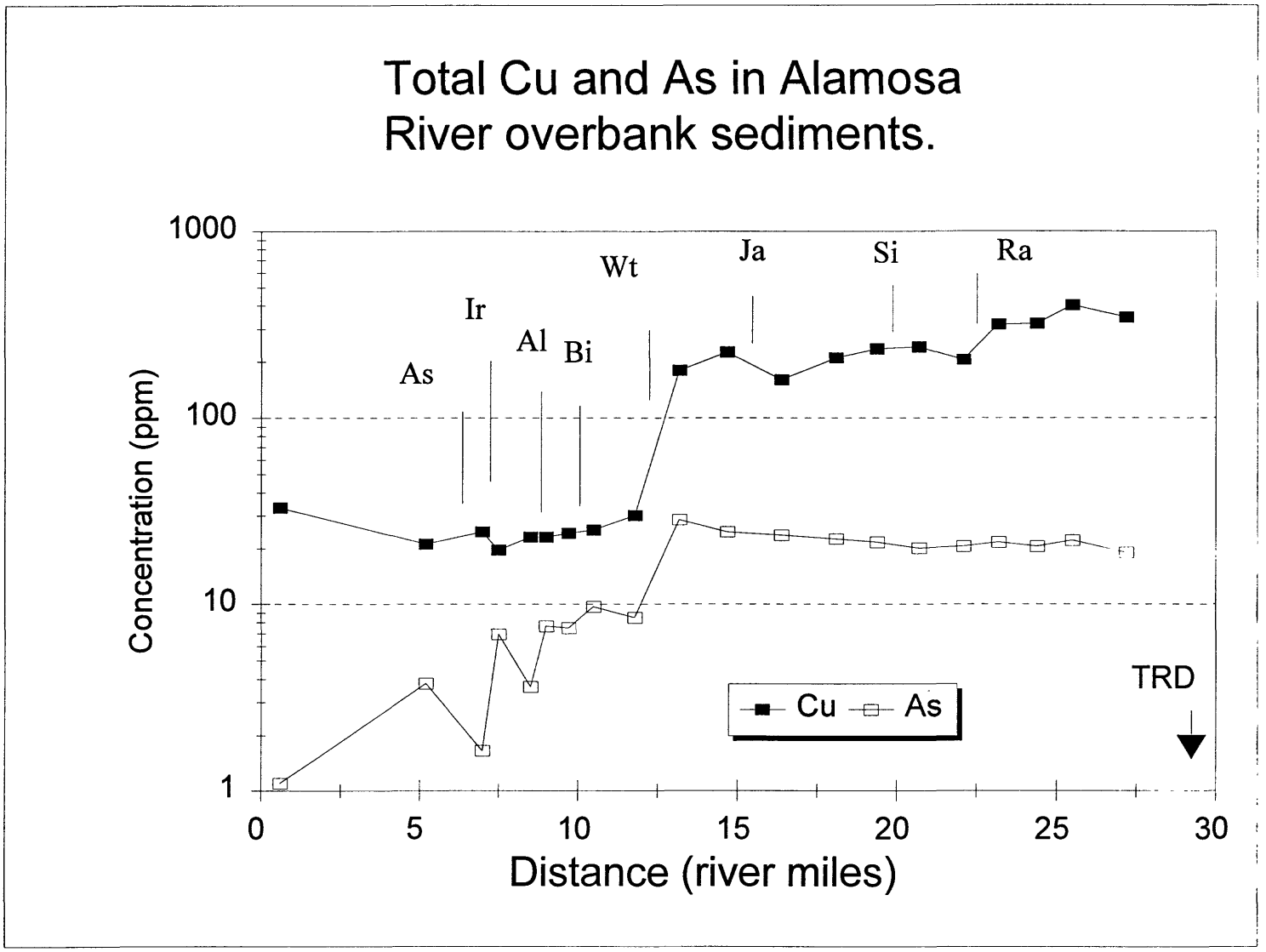

Figure 2. Total copper and arsenic in Alamosa River overbank sediments. Distances are shown in river miles. Tributary inflows are shown as follows: As--Asiatic Creek; Ir--Iron Creek; Al--Alum Creek; Bi--Bitter Creek; Wt--Wightman Fork; Ja--Jasper Creek; Si--Silver Creek; Ra--Ranger Creek. The location of Terrace Reservoir dam is shown by TRD

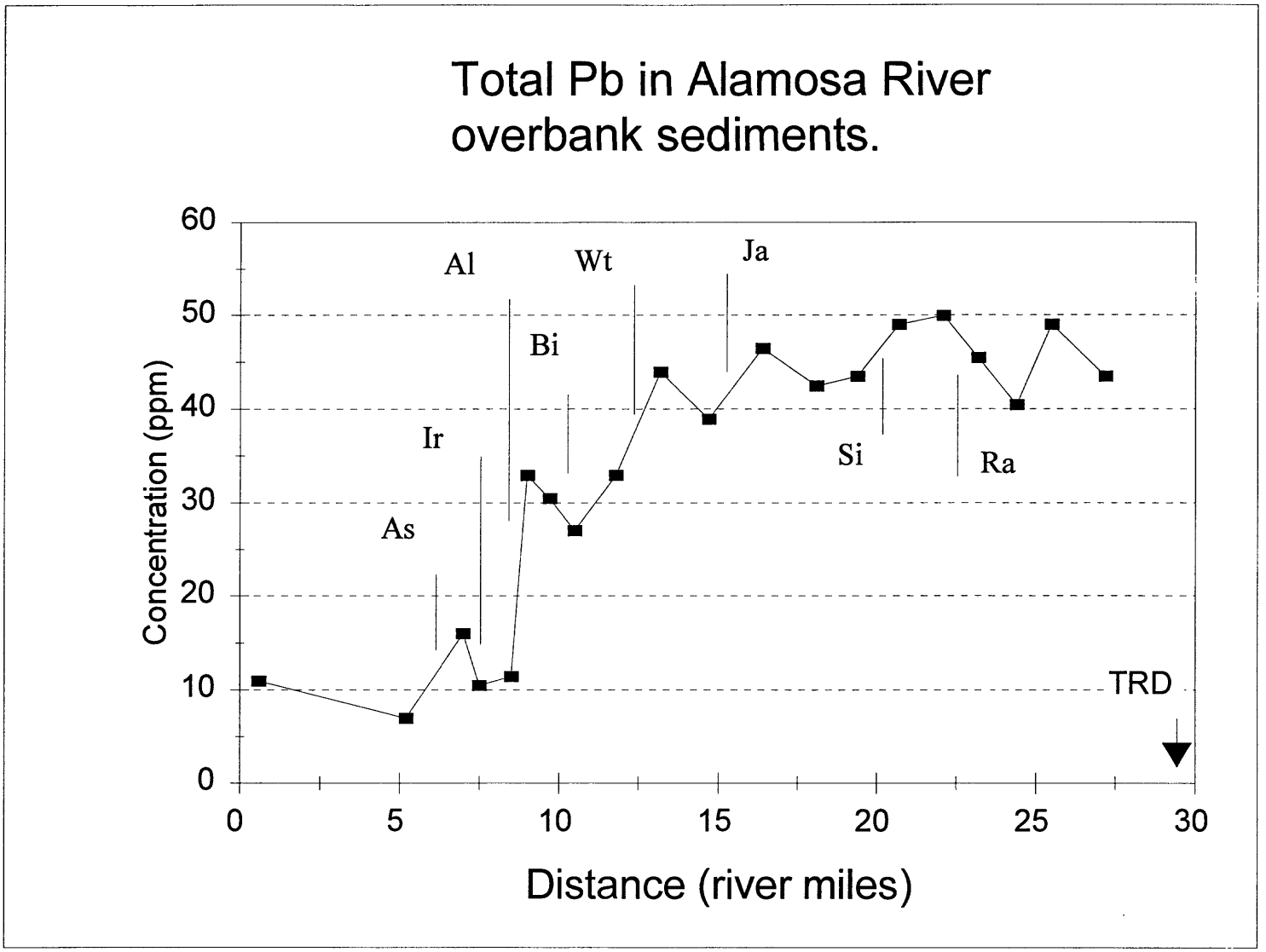

Figure 3. Total lead in Alamosa River overbank sediments. Abbreviations are identical to fig. 2.

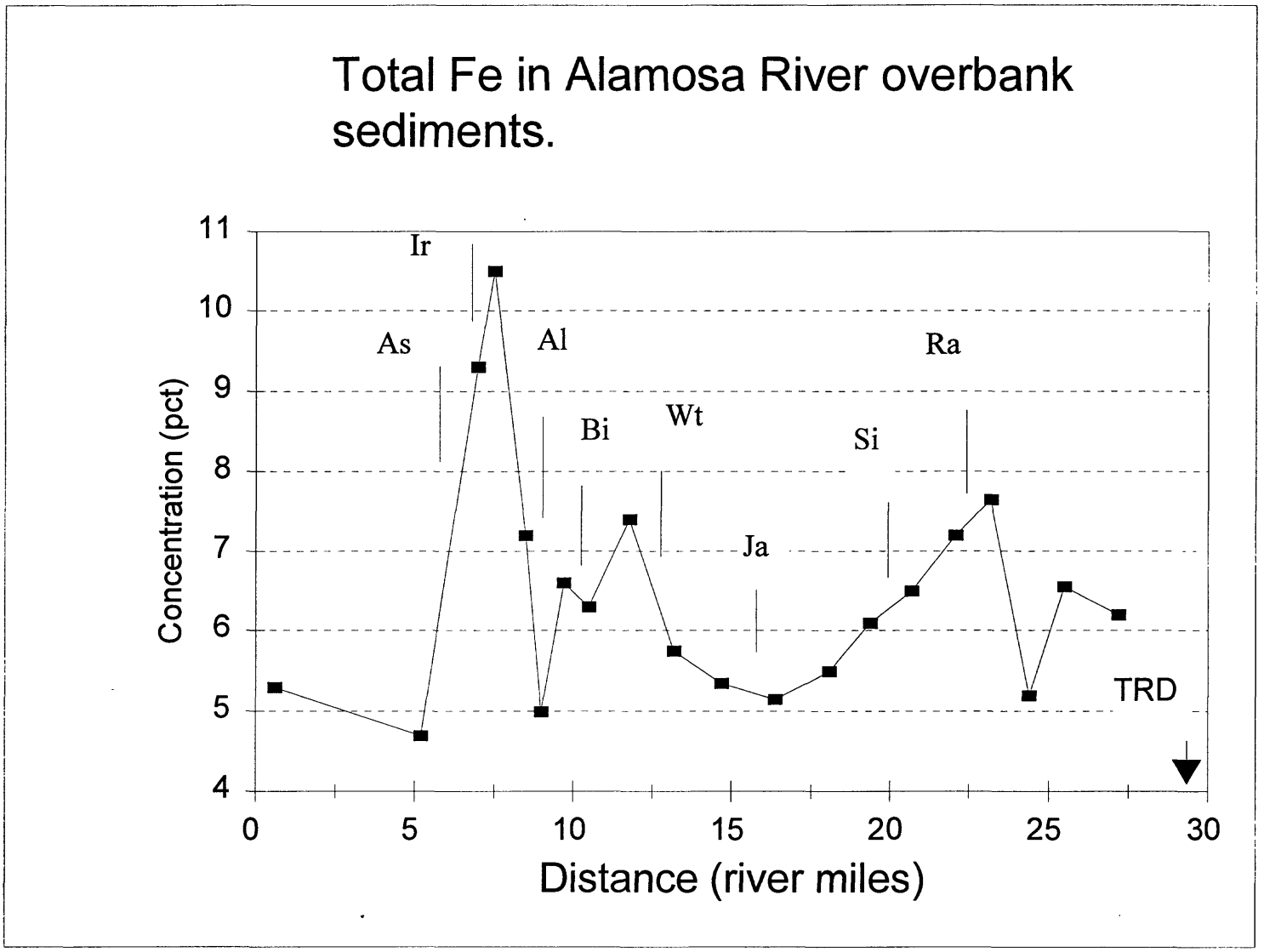

Figure 4. Total iron in Alamosa River overbank sediments. Abbreviations are identical to fig. 2.

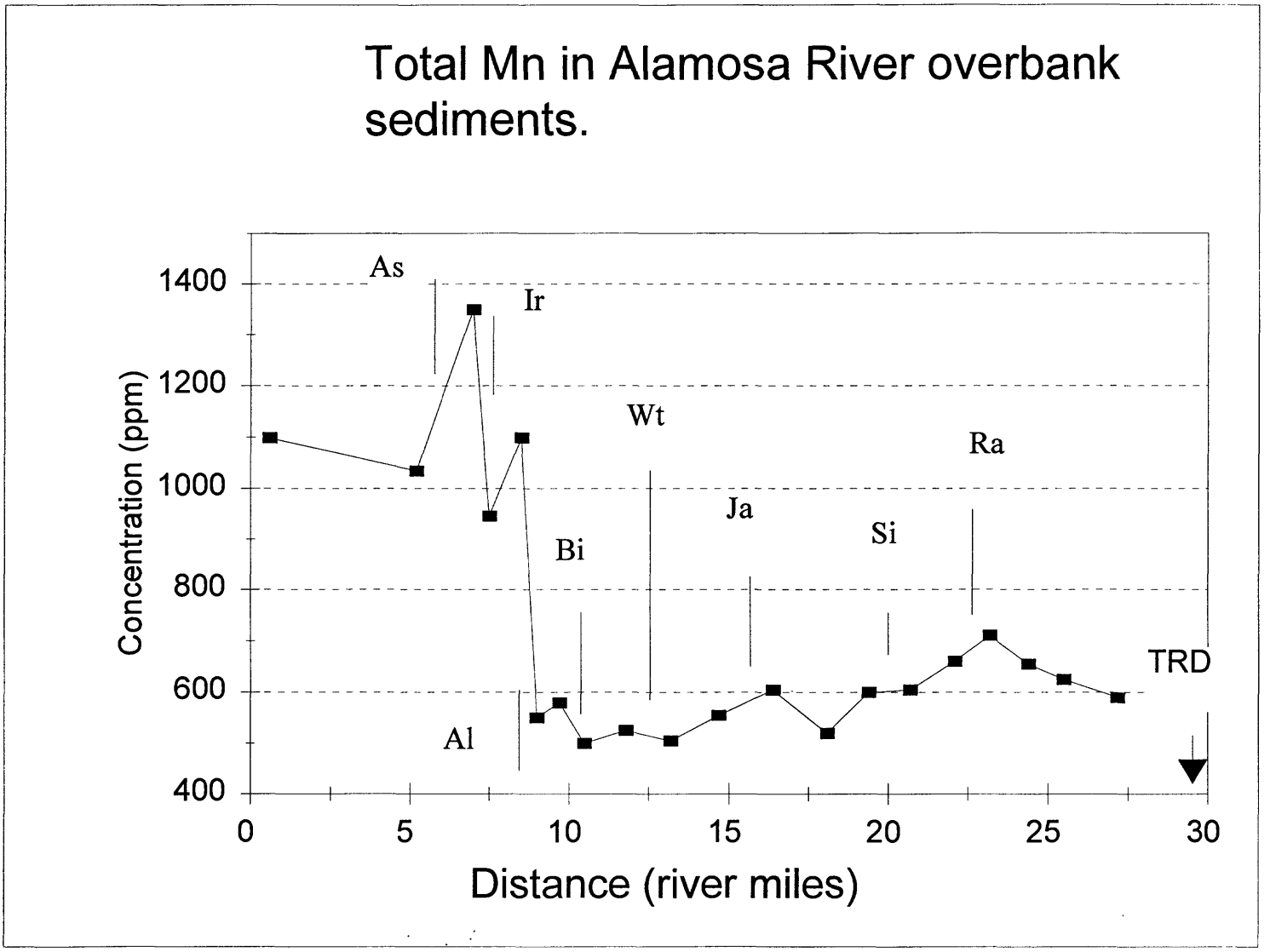

Figure 5. Total manganese in Alamosa River overbank sediments. Abbreviations are identical to fig. 2.

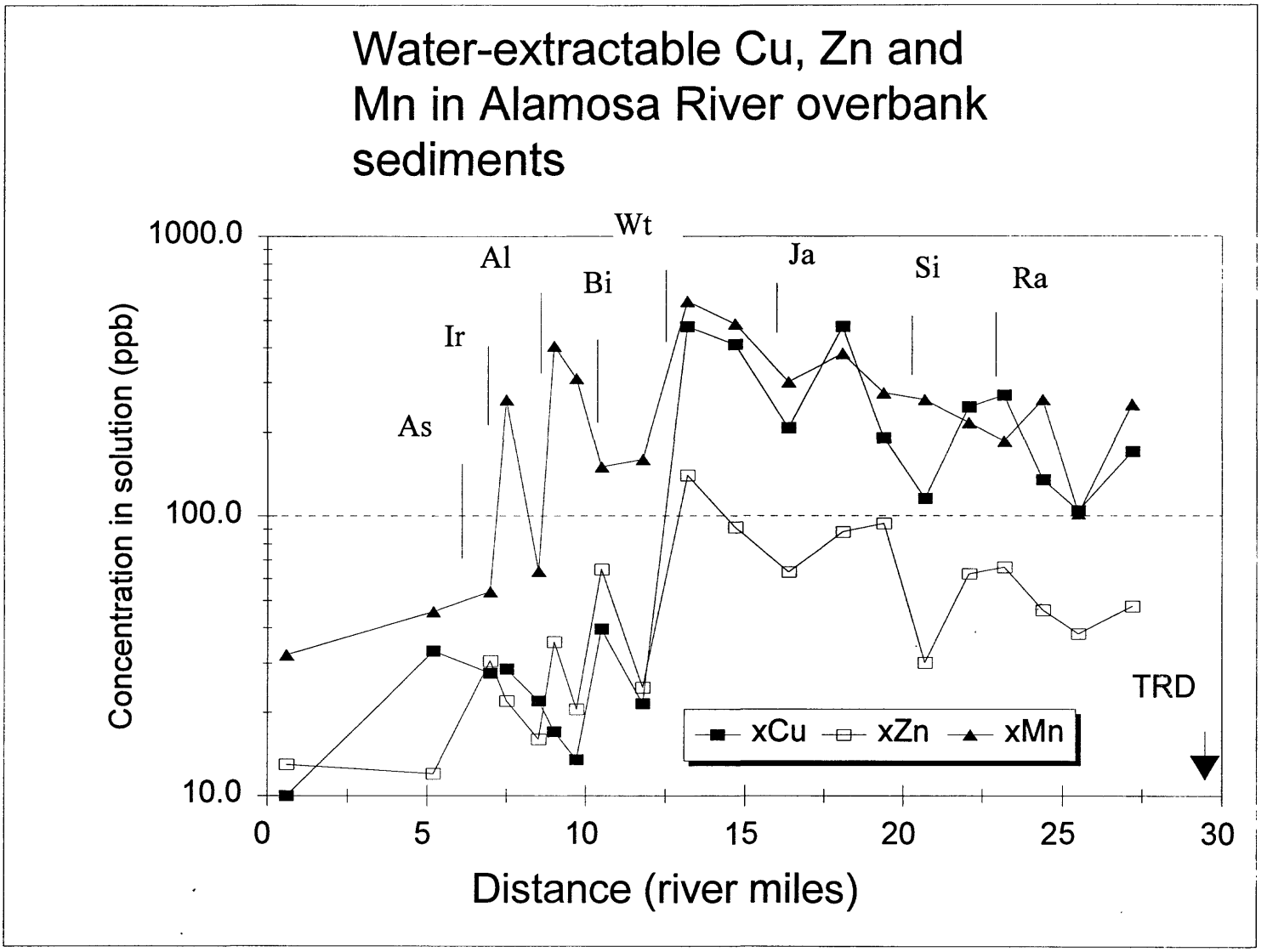

Figure 6. Water-extractable copper, zinc, and manganese in Alamosa River overbank sediments. Abbreviations are identical to fig. 2.

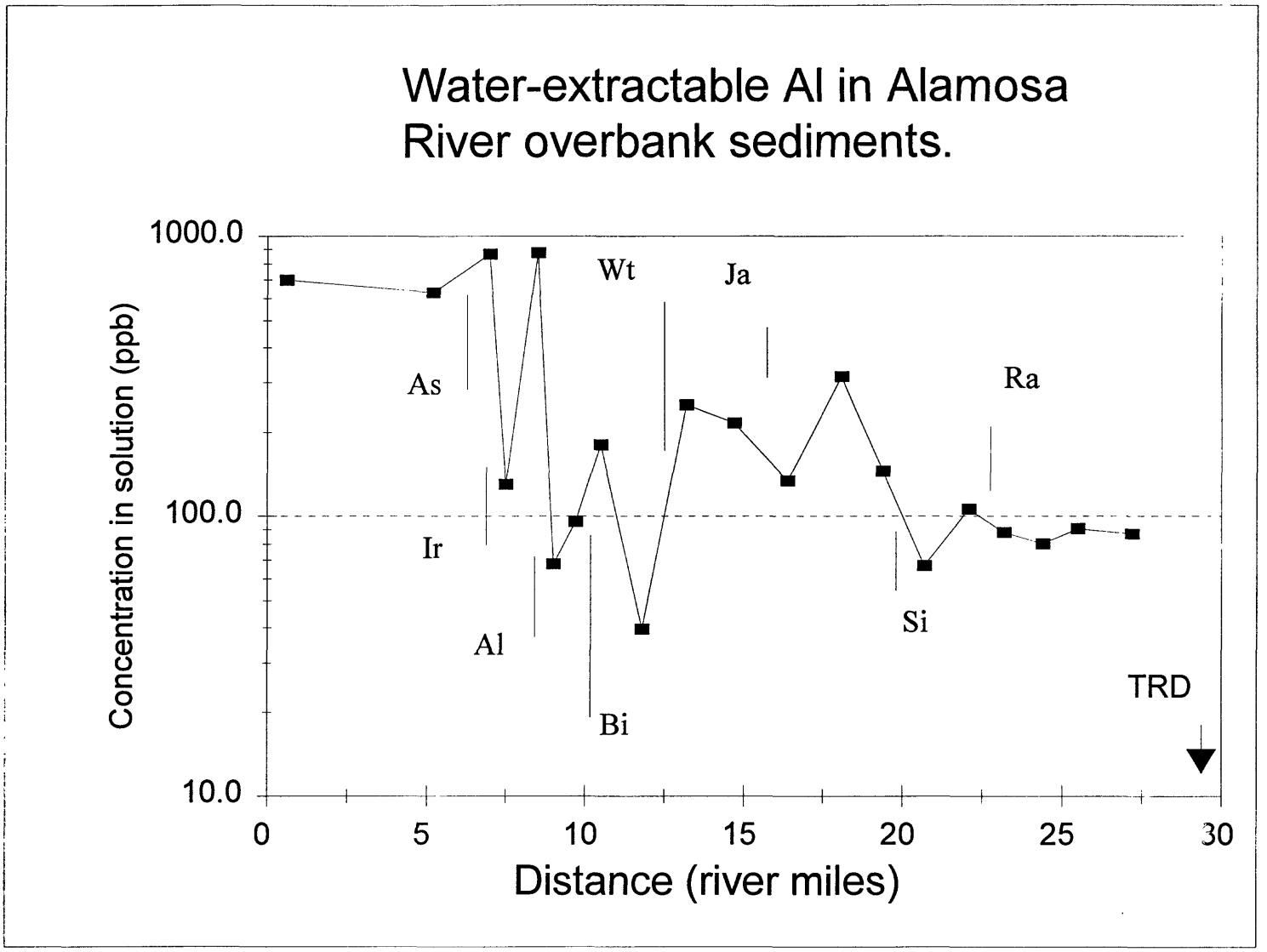

Figure 7. Water-extractable aluminum in Alamosa River overbank sediments. Abbreviations are identical to fig. 2.

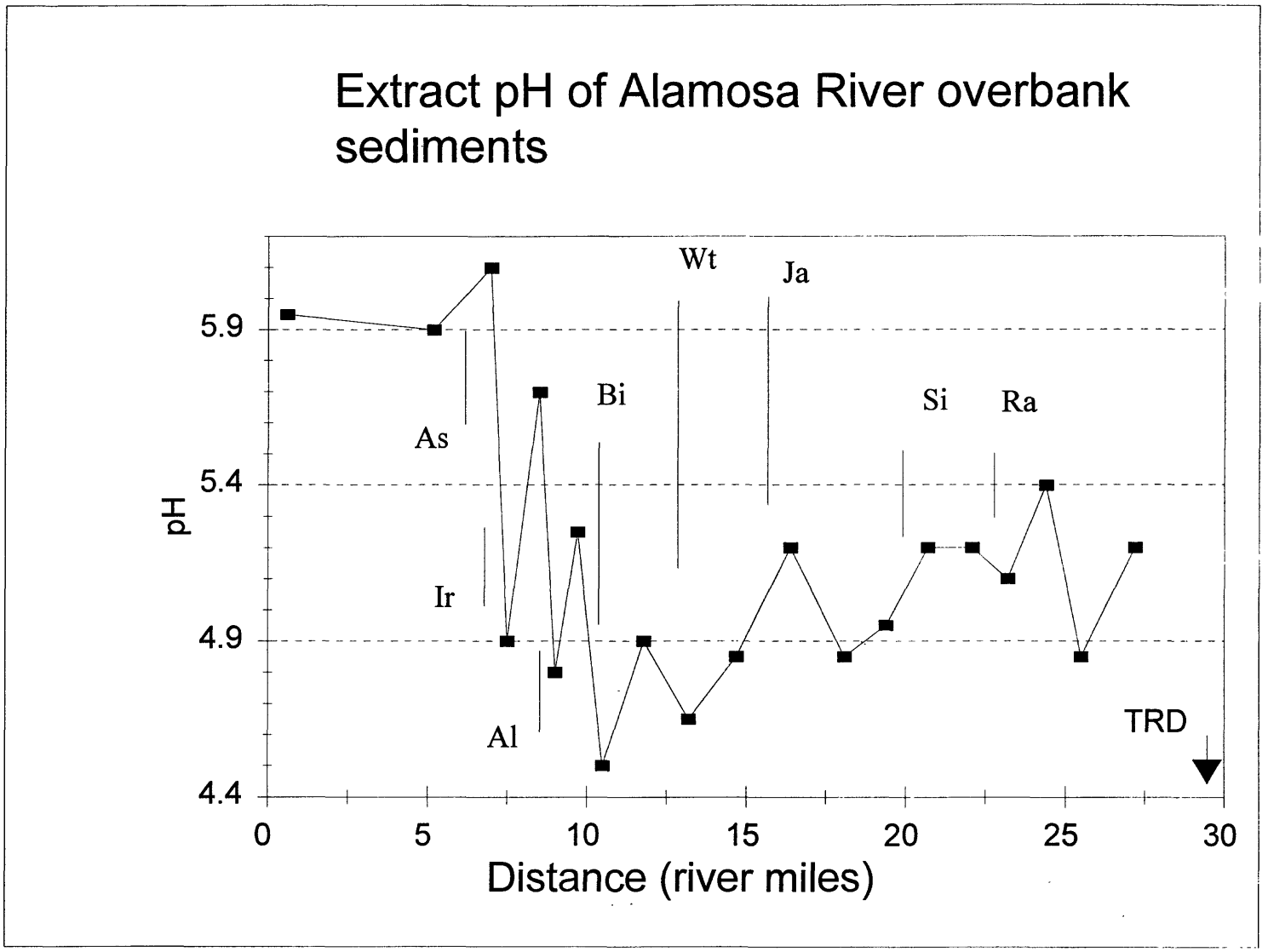

Figure 8. Extract pH of Alamosa River overbank sediments. Abbreviations are identical to fig. 2.

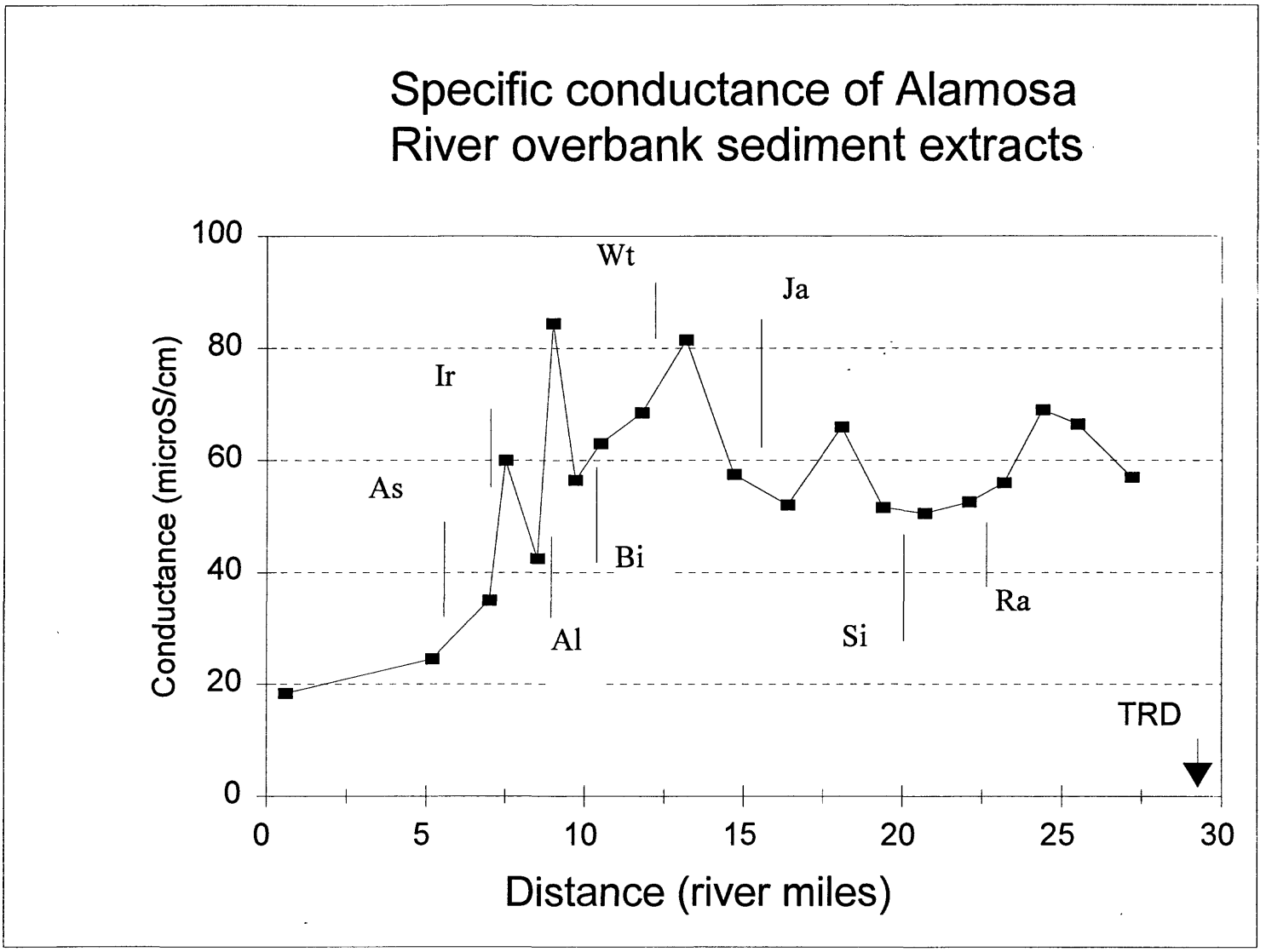

Figure 9. Specific conductance of Alamosa River overbank sediment extracts. Abbreviations are identical to fig. 2.

Table A1. Total element concentrations in Alamosa River overbank sediments determined by ICP-AES.

Field No.	Latitude	Longitude	Al, %	Ca, %	Fe, %	K, %	Mg, %	Na, %	P, %	Ti, %
AR0111	372222	1061931	7.4	0.89	5.7	2.0	0.76	1.2	0.14	0.53
AR0121	372224	1061929	7.4	0.95	6.5	2.0	0.78	1.2	0.13	0.61
AR0122	372224	1061929	7.4	0.95	6.7	2.1	0.78	1.2	0.14	0.62
AR0211	372249	1062050	7.5	1.00	6.3	2.1	0.80	1.3	0.14	0.58
AR0221	372249	1062050	7.2	0.98	6.8	2.0	0.80	1.2	0.13	0.64
AR0222	372249	1062050	7.3	0.98	6.8	2.0	0.80	1.2	0.13	0.64
AR0311	372257	1062139	7.6	0.94	5.8	2.1	0.79	1.2	0.14	0.50
AR0312	372257	1062139	7.5	0.92	5.7	2.1	0.78	1.2	0.14	0.49
AR0321	372257	1062139	7.3	0.92	6.6	2.0	0.78	1.2	0.14	0.64
AR0411	372324	1062235	7.5	0.93	7.3	2.0	0.82	1.2	0.14	0.66
AR0421	372324	1062235	7.4	0.96	8.0	2.0	0.82	1.2	0.14	0.71
AR0511	372324	1062345	7.0	0.97	7.5	2.0	0.81	1.2	0.14	0.74
AR0521	372324	1062345	7.2	0.89	6.9	2.0	0.78	1.2	0.14	0.64
AR0611	372331	1062450	7.3	0.91	5.9	2.0	0.78	1.2	0.14	0.58
AR0621	372331	1062450	7.4	0.92	7.0	2.1	0.79	1.2	0.14	0.62
AR0711	372347	1062553	7.2	0.94	6.3	2.0	0.78	1.2	0.14	0.59
AR0721	372347	1062553	7.5	0.89	5.9	2.0	0.76	1.2	0.14	0.50
AR0811	372409	1062701	7.4	0.92	5.5	2.1	0.76	1.1	0.14	0.49
AR0821	372409	1062701	7.3	0.86	5.4	2.0	0.74	1.1	0.14	0.47
AR0822	372409	1062701	7.5	0.88	5.5	2.0	0.76	1.1	0.14	0.44
AR0911	372459	1062807	7.7	0.85	5.2	2.1	0.76	1.3	0.14	0.44
AR0921	372459	1062807	7.3	0.83	5.1	2.0	0.73	1.1	0.14	0.50
AR1011	372511	1062923	7.7	1.10	5.4	2.0	0.78	1.1	0.13	0.43
AR1021	372511	1062923	7.8	1.20	5.3	2.1	0.82	1.1	0.14	0.47
AR1111	372435	1063018	7.3	1.10	5.9	2.0	0.72	1.0	0.14	0.46
AR1121	372435	1063018	7.4	0.98	5.6	2.0	0.70	1.1	0.14	0.40
AR1211	372404	1063123	6.8	0.96	7.8	1.8	0.73	0.8	0.13	0.43
AR1221	372404	1063123	7.2	1.30	7.0	1.9	0.77	0.9	0.12	0.41
AR1222	372404	1063123	7.3	1.30	7.0	1.9	0.79	0.9	0.13	0.42
AR1311	372337	1063229	7.6	1.00	6.8	2.0	0.80	0.9	0.16	0.40
AR1312	372337	1063229	7.3	1.00	6.5	2.0	0.79	0.9	0.16	0.44
AR1321	372337	1063229	7.5	1.20	5.8	2.0	0.82	1.0	0.13	0.42
AR1411	372335	1063319	6.9	1.50	8.1	1.8	0.86	0.9	0.13	0.65
AR1421	372335	1063319	7.3	1.40	5.0	1.9	0.79	0.9	0.12	0.43
AR1511	372304	1063350	7.7	1.50	4.7	2.0	0.86	0.9	0.13	0.44
AR1512	372304	1063350	8.2	1.50	4.8	2.1	0.88	1.0	0.13	0.39
AR1521	372304	1063350	7.5	1.40	5.3	2.0	0.84	0.9	0.13	0.44
AR1611	372246	1063415	8.5	2.80	7.3	1.8	1.20	1.6	0.14	0.69
AR1621	372246	1063415	8.6	2.60	7.1	1.8	1.10	1.5	0.14	0.65
AR1711	372159	1063902	9.3	4.40	5.3	1.6	1.50	2.1	0.13	0.52
AR1721	372159	1063902	8.9	4.40	5.3	1.5	1.50	2.0	0.13	0.54
AR1811	372105	1063542	7.8	1.50	5.0	2.3	0.91	1.2	0.12	0.62
AR1821	372105	1063542	8.1	1.50	4.4	2.3	0.96	1.2	0.12	0.54
AR1911	372204	1063514	8.6	3.60	9.0	1.6	1.40	1.8	0.14	0.91
AR1921	372204	1063514	8.5	3.50	9.5	1.6	1.40	1.8	0.14	0.93
AR2011	372226	1063450	8.1	1.60	10.0	1.8	0.97	1.2	0.15	0.94
AR2012	372226	1063450	7.9	1.70	11.0	1.7	0.97	1.2	0.15	0.95
AR2021	372226	1063450	7.7	1.30	9.3	1.7	0.90	1.1	0.15	0.82

Table A1 cont.

Field No.	Latitude	Longitude	As, ppm	Ba, ppm	Be, ppm	Ce, ppm	Co, ppm,	Cr, ppm	Cu, ppm
AR0111	372222	1061931	14	900	2	61	14	20	340
AR0121	372224	1061929	16	940	2	53	17	23	350
AR0122	372224	1061929	14	870	2	54	17	24	350
AR0211	372249	1062050	14	990	2	53	15	23	400
AR0221	372249	1062050	16	1000	2	60	17	25	400
AR0222	372249	1062050	17	920	2	59	16	27	400
AR0311	372257	1062139	18	810	2	53	16	20	340
AR0312	372257	1062139	16	850	2	52	16	20	340
AR0321	372257	1062139	19	1000	2	60	17	24	300
AR0411	372324	1062235	16	1100	2	53	17	26	320
AR0421	372324	1062235	11	1200	2	54	18	30	310
AR0511	372324	1062345	23	1200	2	63	17	27	180
AR0521	372324	1062345	18	1100	2	57	16	26	230
AR0611	372331	1062450	16	930	2	61	14	20	260
AR0621	372331	1062450	14	1000	2	51	16	25	220
AR0711	372347	1062553	15	1000	2	59	16	22	210
AR0721	372347	1062553	15	860	1	53	14	20	260
AR0811	372409	1062701	16	870	2	59	13	19	210
AR0821	372409	1062701	17	840	1	58	12	17	210
AR0822	372409	1062701	15	880	1	52	14	15	220
AR0911	372459	1062807	14	830	1	53	17	16	130
AR0921	372459	1062807	18	790	1	60	12	17	190
AR1011	372511	1062923	16	480	1	52	14	15	230
AR1021	372511	1062923	18	850	1	59	13	17	220
AR1111	372435	1063018	18	740	1	58	13	14	190
AR1121	372435	1063018	19	690	1	51	12	12	170
AR1211	372404	1063123	10	320	1	55	15	14	25
AR1221	372404	1063123	10	150	1	48	17	14	35
AR1222	372404	1063123	10	140	1	50	16	14	25
AR1311	372337	1063229	<10	630	1	47	11	15	25
AR1312	372337	1063229	<10	690	1	55	11	14	25
AR1321	372337	1063229	<10	830	1	46	12	14	25
AR1411	372335	1063319	<10	150	1	61	19	19	25
AR1421	372335	1063319	<10	630	1	60	13	12	23
AR1511	372304	1063350	<10	790	1	61	11	12	19
AR1512	372304	1063350	<10	580	1	52	12	12	22
AR1521	372304	1063350	<10	370	1	53	13	12	27
AR1611	372246	1063415	<10	880	1	50	22	14	24
AR1621	372246	1063415	<10	790	1	53	22	14	22
AR1711	372159	1063902	<10	680	1	54	19	9	20
AR1721	372159	1063902	<10	650	1	52	20	9	19
AR1811	372105	1063542	<10	720	1	69	16	19	24
AR1821	372105	1063542	<10	740	2	68	15	18	25
AR1911	372204	1063514	<10	660	1	53	27	15	24
AR1921	372204	1063514	<10	670	1	58	29	17	18
AR2011	372226	1063450	<10	940	1	58	24	31	34
AR2012	372226	1063450	<10	830	1	55	25	27	33
AR2021	372226	1063450	<10	1400	1	61	21	25	32

Table A1 cont.

Field No.	Latitude	Longitude	Ga, ppm	La, ppm	Li, ppm	Mn, ppm	Nb, ppm	Nd, ppm	Ni, ppm
AR0111	372222	1061931	18	33	11	540	18	29	9
AR0121	372224	1061929	18	30	11	640	16	27	11
AR0122	372224	1061929	18	30	11	660	17	26	11
AR0211	372249	1062050	18	30	11	610	16	24	11
AR0221	372249	1062050	19	32	10	640	17	29	10
AR0222	372249	1062050	18	32	10	650	18	28	11
AR0311	372257	1062139	19	30	10	630	16	25	9
AR0312	372257	1062139	17	29	10	610	16	26	10
AR0321	372257	1062139	19	32	11	680	20	26	10
AR0411	372324	1062235	18	29	10	690	17	25	11
AR0421	372324	1062235	19	29	10	730	17	25	12
AR0511	372324	1062345	20	33	10	690	16	29	11
AR0521	372324	1062345	18	31	10	630	18	27	10
AR0611	372331	1062450	17	33	10	560	19	27	8
AR0621	372331	1062450	17	29	10	650	16	24	10
AR0711	372347	1062553	18	31	10	620	17	27	9
AR0721	372347	1062553	18	30	10	580	16	25	10
AR0811	372409	1062701	19	32	10	540	17	30	9
AR0821	372409	1062701	17	32	10	500	17	28	7
AR0822	372409	1062701	17	29	10	540	15	25	7
AR0911	372459	1062807	17	30	11	700	16	26	8
AR0921	372459	1062807	18	34	10	510	19	29	7
AR1011	372511	1062923	18	29	10	550	15	24	8
AR1021	372511	1062923	18	33	10	560	16	28	7
AR1111	372435	1063018	17	32	10	500	16	28	7
AR1121	372435	1063018	16	29	9	510	15	25	6
AR1211	372404	1063123	17	30	8	460	15	26	7
AR1221	372404	1063123	16	27	8	590	14	23	8
AR1222	372404	1063123	16	27	8	580	13	24	9
AR1311	372337	1063229	18	27	10	490	15	22	6
AR1312	372337	1063229	18	31	10	470	17	26	6
AR1321	372337	1063229	18	26	8	510	15	22	6
AR1411	372335	1063319	19	32	8	650	17	28	9
AR1421	372335	1063319	17	33	7	510	16	28	7
AR1511	372304	1063350	19	33	8	560	16	30	6
AR1512	372304	1063350	19	30	9	600	15	26	5
AR1521	372304	1063350	17	30	8	540	14	25	6
AR1611	372246	1063415	20	27	12	1100	19	25	8
AR1621	372246	1063415	20	28	13	1100	18	28	8
AR1711	372159	1063902	21	28	15	1100	18	25	7
AR1721	372159	1063902	21	27	13	1100	19	26	7
AR1811	372105	1063542	19	37	17	1100	22	32	9
AR1821	372105	1063542	19	37	19	970	21	32	9
AR1911	372204	1063514	22	27	12	1300	19	25	9
AR1921	372204	1063514	25	28	13	1400	17	26	9
AR2011	372226	1063450	22	29	10	1000	18	26	12
AR2012	372226	1063450	22	28	10	1100	19	25	12
AR2021	372226	1063450	21	30	9	890	18	28	9

Table A1 cont.

Field No.	Latitude	Longitude	Pb, ppm	Sc, ppm	Sr, ppm	Th, ppm	V, ppm	Y, ppm	Zn, ppm
AR0111	372222	1061931	44	11	380	10	140	12	110
AR0121	372224	1061929	43	11	380	8	170	11	140
AR0122	372224	1061929	42	11	390	8	180	11	140
AR0211	372249	1062050	45	11	400	7	160	11	130
AR0221	372249	1062050	53	11	380	9	180	12	140
AR0222	372249	1062050	55	11	380	9	180	11	140
AR0311	372257	1062139	43	11	380	8	140	11	120
AR0312	372257	1062139	38	11	370	8	140	11	120
AR0321	372257	1062139	58	11	380	9	170	11	160
AR0411	372324	1062235	48	11	380	7	180	11	140
AR0421	372324	1062235	43	12	380	9	210	10	160
AR0511	372324	1062345	51	12	390	10	200	12	140
AR0521	372324	1062345	49	11	380	8	180	11	130
AR0611	372331	1062450	45	11	380	9	150	12	110
AR0621	372331	1062450	53	11	360	8	180	10	130
AR0711	372347	1062553	50	11	370	10	160	11	120
AR0721	372347	1062553	37	11	360	8	140	11	120
AR0811	372409	1062701	43	11	370	10	130	11	92
AR0821	372409	1062701	42	11	360	10	130	12	91
AR0822	372409	1062701	35	11	350	8	130	11	91
AR0911	372459	1062807	45	11	390	8	120	11	99
AR0921	372459	1062807	48	11	370	10	120	13	81
AR1011	372511	1062923	35	11	350	7	120	12	92
AR1021	372511	1062923	43	11	370	10	120	13	87
AR1111	372435	1063018	41	11	350	9	120	12	85
AR1121	372435	1063018	47	11	350	8	120	11	98
AR1211	372404	1063123	30	11	310	9	130	10	70
AR1221	372404	1063123	36	11	330	9	130	10	96
AR1222	372404	1063123	25	11	340	8	130	11	91
AR1311	372337	1063229	30	12	310	8	130	10	70
AR1312	372337	1063229	32	12	320	11	130	11	68
AR1321	372337	1063229	24	12	340	9	130	10	71
AR1411	372335	1063319	29	13	360	10	180	13	100
AR1421	372335	1063319	32	11	380	9	120	12	69
AR1511	372304	1063350	33	12	390	10	120	13	66
AR1512	372304	1063350	28	12	390	8	110	12	67
AR1521	372304	1063350	33	12	360	8	130	11	70
AR1611	372246	1063415	11	14	500	6	180	17	130
AR1621	372246	1063415	12	14	480	5	170	18	130
AR1711	372159	1063902	10	15	670	5	120	21	96
AR1721	372159	1063902	11	16	650	4	130	21	96
AR1811	372105	1063542	17	12	320	7	130	20	100
AR1821	372105	1063542	15	12	320	9	110	21	92
AR1911	372204	1063514	7	17	550	11	240	20	160
AR1921	372204	1063514	7	16	540	4	260	19	160
AR2011	372226	1063450	8	14	420	5	260	14	170
AR2012	372226	1063450	12	14	410	5	270	14	170
AR2021	372226	1063450	14	13	370	6	220	14	130

Table A2. Total arsenic concentration in overbank sediments from the Alamosa River determined by hydride-generation atomic absorption spectrocsopy (HGAA)

Field No.	Latitude	Longitude	As, ppm
AR0111	372222	1061931	20
AR0121	372224	1061929	18
AR0122	372224	1061929	17
AR0211	372249	1062050	20
AR0221	372249	1062050	24
AR0222	372249	1062050	21
AR0311	372257	1062139	22
AR0312	372257	1062139	21
AR0321	372257	1062139	19
AR0411	372324	1062235	24
AR0421	372324	1062235	19
AR0511	372324	1062345	21
AR0521	372324	1062345	20
AR0611	372331	1062450	20
AR0621	372331	1062450	20
AR0711	372347	1062553	21
AR0721	372347	1062553	22
AR0811	372409	1062701	24
AR0821	372409	1062701	21
AR0822	372409	1062701	22
AR0911	372459	1062807	23
AR0921	372459	1062807	24
AR1011	372511	1062923	23
AR1021	372511	1062923	26
AR1111	372435	1063018	28
AR1121	372435	1063018	29
AR1211	372404	1063123	9
AR1221	372404	1063123	8
AR1222	372404	1063123	8
AR1311	372337	1063229	11
AR1312	372337	1063229	11
AR1321	372337	1063229	9
AR1411	372335	1063319	8
AR1421	372335	1063319	7
AR1511	372304	1063350	8
AR1512	372304	1063350	8
AR1521	372304	1063350	8
AR1611	372246	1063415	3
AR1621	372246	1063415	4
AR1711	372159	1063902	1
AR1721	372159	1063902	1
AR1811	372105	1063542	4
AR1821	372105	1063542	4
AR1911	372204	1063514	2
AR1921	372204	1063514	2
AR2011	372226	1063450	6
AR2012	372226	1063450	6
AR2021	372226	1063450	8

Table A3. Water-extractable constituents in overbank sediments from the Alamosa River. Values are in 1:20 sediment:water leachate. SC= specific conductance.

Field No	Al ppb	Ba ppb	Cu ppb	Mg ppb	Mn ppb	Zn ppb	pH	SC, microS/cm
AR0111x	99	40	190	800	260	53	5.0	61
AR0121x	74	35	150	690	240	42	5.3	53
AR0122x	100	34	160	710	240	45	5.0	54
AR0211x	85	79	49	570	54	16	5.5	63
AR0221x	96	37	160	1000	150	60	4.2	70
AR0222x	63	40	110	730	130	40	5.0	39
AR0311x	50	35	100	830	270	45	5.6	72
AR0312x	50	36	92	800	280	59	5.4	66
AR0321x	110	45	170	700	250	47	5.2	35
AR0411x	88	50	300	740	180	66	5.1	55
AR0421x	87	56	240	630	190	65	5.1	57
AR0511x	82	53	180	600	210	55	5.0	49
AR0521x	130	60	310	730	220	69	5.1	56
AR0611x	59	36	81	690	260	26	5.3	43
AR0621x	74	41	150	660	260	34	5.1	58
AR0711x	170	45	180	670	230	120	4.9	30
AR0721x	120	66	200	830	320	68	5.0	73
AR0811x	260	48	310	870	400	76	5.0	62
AR0821x	370	60	640	840	360	99	4.7	70
AR0822x	340	58	600	890	340	99	4.7	80
AR0911x	68	48	52	490	200	32	5.1	45
AR0921x	200	50	360	800	400	94	5.3	59
AR1011x	180	47	340	900	440	82	4.9	74
AR1021x	250	56	480	1000	530	100	4.8	41
AR1111x	280	65	520	1800	570	160	4.7	72
AR1121x	220	64	430	1100	600	120	4.6	91
AR1211x	58	50	38	1200	150	34	4.8	57
AR1221x	54	40	5	1200	170	28	5.0	80
AR1222x	21	44	20	1100	150	15	5.0	69
AR1311x	130	42	21	740	170	42	4.4	73
AR1312x	180	43	23	700	180	41	4.6	53
AR1321x	230	44	58	720	130	87	4.6	53
AR1411x	120	59	12	2400	350	24	5.2	69
AR1421x	72	41	15	1300	270	17	5.3	44
AR1511x	58	66	10	1500	390	32	4.8	75
AR1512x	110	73	12	1700	450	84	4.9	98
AR1521x	77	65	24	1300	420	39	4.8	94
AR1611x	550	39	22	890	68	10	5.9	53
AR1621x	1200	24	22	560	59	22	5.5	32
AR1711x	780	9	37	580	34	9.0	6.0	20
AR1721x	620	8	20	550	30	17	5.9	17
AR1811x	580	25	41	780	48	14	5.8	20
AR1821x	680	18	14	640	43	10	6.0	29
AR1911x	830	24	54	940	48	33	6.2	42
AR1921x	900	27	12	770	59	28	6.0	28
AR2011x	140	62	14	1100	230	30	5.0	63
AR2012x	100	57	18	1000	230	20	5.2	57
AR2021x	120	53	6	1000	290	14	4.8	59